

Automatic Design of Transonic Airfoils to Reduce
Reduce the Shock Induced Pressure Drag

Antony Jameson

Princeton University
MAE Report 1881

As presented at the 31st Israel Annual Conference
on Aviation and Aeronautics
February 21-22, 1990

AUTOMATIC DESIGN OF TRANSONIC AIRFOILS TO REDUCE THE SHOCK INDUCED PRESSURE DRAG

Antony Jameson
Princeton University
Princeton, New Jersey, USA

Abstract

This paper discusses the use of control theory for optimum design of aerodynamic configurations. Examples are presented of the application of this method to the reduction of shock induced pressure drag on airfoils in two-dimensional transonic flow.

1 Introduction

Prior to 1960, computational methods were hardly used in aerodynamic analysis. The primary tool for the development of aerodynamic configurations was the wind tunnel. Shapes were tested and modifications selected in the light of pressure and force measurements together with flow visualization techniques. Computational methods are now quite widely accepted in the aircraft industry. This has been brought about by a combination of radical improvements in numerical algorithms and continuing advances in both speed and memory of computers.

If a computational method is to be useful in the design process, it must be based on a mathematical model which provides an appropriate representation of the significant features of the flow, such as shock waves, vortices and boundary layers. The method must also be robust, not liable to fail when parameters are varied, and it must be able to treat useful configurations, ultimately the complete aircraft. Finally, reasonable accuracy should be attainable at reasonable cost. Much progress has been made in these directions [1, 2, 3, 4, 5, 6, 7, 8, 9, 10]. In many applications where the flow is unseparated, including designs for transonic flow with weak shock waves, useful predictions can be made quite inexpensively using the potential flow equation [1, 2, 3, 4]. Methods are also available for solving the Euler equations for two- and three- dimensional configurations up to a complete aircraft [5, 6, 7, 8, 9, 10]. Viscous simulations are generally complicated by the need to allow for turbulence: while the Reynolds averaged equations can be solved by current methods, the results

depend heavily on the choice of turbulence models. Assuming that one has the ability to predict the performance of a given design, the question then arises of how to modify it to attain significant improvements in its performance.

Given the range of well proven methods now available, one can thus distinguish objectives for computational aerodynamics at several levels:

1. Capability to predict the flow past an airplane or important components in different flight regimes such as take-off or cruise, and off-design conditions such as flutter.
2. Interactive design calculations to allow rapid improvement of the design.
3. Automatic design optimization.

Substantial progress has been made toward the first objective, and in relatively simple cases such as an airfoil or wing in inviscid flow, calculations can be performed fast enough that the second objective is within reach. The subtlety and complexity of fluid flow is such that it is unlikely that interactive trials can lead to a truly optimum design. Eventually, therefore, one should aim to have automatic optimization procedures built into the design process. This is the third objective. Progress has been inhibited by the extreme computing costs that might be incurred, but useful design methods have been devised for various simplified cases such as two-dimensional airfoils and cascades, and wings in potential flow.

In particular, it has been recognized that the designer generally has an idea of the kind of pressure distribution that will lead to the desired performance. Thus, it is useful to consider the problem of calculating the shape that will lead to a given pressure distribution in steady flow. Such a shape does not necessarily exist, unless the pressure distribution satisfies certain constraints, and the problem must therefore be very carefully formulated: no shape exists, for example, for which stagnation pressure is attained

over the entire surface. The problem of designing a two-dimensional profile to attain a desired pressure distribution was first studied by Lighthill, who solved it for the case of incompressible flow by conformally mapping the profile to a unit circle [11]. The speed over the profile is

$$q = \phi_\theta/h \quad (1)$$

where ϕ is the potential for flow past a circle, and h is the modulus of the mapping function. The solution for ϕ is known for incompressible flow. Let q_d be the desired surface speed. The surface value of h can be obtained by setting $q = q_d$ in Equation 1, and since the mapping function is analytic, it is uniquely determined by the value of h on the boundary. A solution exists for a given speed q_∞ at infinity only if

$$\frac{1}{2\pi} \oint q d\theta = q_\infty \quad (2)$$

and there are additional constraints on q if the profile is required to be closed.

Lighthill's method was extended to compressible flow by McFadden [12]. Starting with a given shape and a corresponding mapping function $h^{(0)}$, the flow equation can be solved for the potential $\phi^{(0)}$, which now depends on $h^{(0)}$. A new mapping function $h^{(1)}$, is then determined by setting $q = q_d$ in Equation 1, and the process is repeated. In the limiting case of zero Mach number, the method reduces to Lighthill's method, and McFadden gives a proof that the iterations will converge for small Mach numbers. He also extends the method to treat transonic flow through introduction of artificial viscosity to suppress the appearance of shock waves, which would cause the updated mapping function to be discontinuous. This difficulty can also be overcome by smoothing the changes in the mapping function. Such an approach is used in a computer program written by the author at Grumman Aerospace. It allows the recovery of smooth profiles that generate flows containing shock waves, and it has been used to design improved blade sections for propeller [13]. A related method for three-dimensional design was devised by Garabedian and McFadden [14]. In their scheme the steady potential flow solution is obtained by solving an artificial time dependent equation, and the surface is treated as a free boundary. This is shifted according to an auxiliary time dependent equation in such a way that the flow evolves toward the specified pressure distribution.

Another way to formulate the problem of designing a profile for a given pressure distribution is to integrate the corresponding surface speed to obtain the surface potential. The potential flow equation is then solved with a Dirichlet boundary condition, and

a shape correction is determined from the calculated normal velocity through the surface. This approach was first tried by Tranen [15]. Volpe and Melnik have shown how to allow for the constraints that must be satisfied by the pressure distribution if a solution is to exist [16]. The same idea has been used by Henne for three-dimensional design calculations [17].

The hodograph approach transformation offers an alternative approach to the design of airfoils in transonic flows. Garabedian and Korn achieved a striking success in the design of airfoils to produce shock-free transonic flows by using the method of complex characteristics to solve the equation in the hodograph plane [18]. Another design procedure has been proposed by Giles, Drela, and Thompkins [19], who write the two-dimensional Euler equations for inviscid flow in a streamline coordinate system, and use a Newton iteration. An option is then provided to treat the surface coordinates as unknowns while the pressure is fixed.

Finally, there have been studies of the possibility of meeting desired design objectives by using constrained optimization [20, 21]. The configuration is specified by a set of parameters, and any suitable computer program for flow analysis is used to evaluate the aerodynamic characteristics. The optimization method then selects values of these parameters that maximize some criterion of merit, such as the lift-to-drag ratio, subject to other constraints such as required wing thickness and volume. In principle, this method allows the designer to specify any reasonable design objectives. The method becomes extremely expensive, however, as the number of parameters is increased, and its successful application in practice depends heavily on the choice of a parametric representation of the configuration.

In a recent paper [22], the author suggested that there are benefits in regarding the design problems as a control problem in which the control is the shape of the boundary. A variety of alternative formulations of the design problem can then be treated systematically by using the mathematical theory for control of systems governed by partial differential equations [23]. Suppose that the boundary is defined by a function $f(\underline{x})$, where \underline{x} is the positive vector. As in the case of optimization theory applied to the design problem, the desired objective is specified by a cost function I , which may for example, measure the deviation from the desired surface pressure distribution, but could also represent other measured of performance such as lift and drag. The introduction of a cost function has the advantage that if the objective is unattainable, it is still possible to find a minimum cost function. Now a variation in the control δf leads to a variable δI in the cost. It is shown

in the following sections that δI can be expressed to first order as an inner product of a gradient function g with δf :

$$\delta I = (g, \delta f) \quad (3)$$

Hence g is independent of the particular variation δf in the control, and can be determined by solving an adjoint equation. Now choose

$$\delta f = -\lambda g \quad (4)$$

where λ is a sufficient small positive number. Then,

$$\delta I = -\lambda (g, g) < 0 \quad (5)$$

assuring a reduction in I . After making such a modification, the gradient can be recalculated and the process repeated to follow a path of steepest descent until a minimum is reached. In order to avoid violating constraints, such as a minimum acceptable wing thickness, the steps can be taken along the projection of the gradient into the allowable subspace of the control function. In this way one can devise design procedures which must necessarily converge at least to a local minimum, and which might be accelerated by the use of more sophisticated descent methods. While there is a possibility of more than one local minimum, the cost function can be chosen to reduce the likelihood of difficulties caused by such a contingency, and in any case the method will lead to an improvement over the initial design. The mathematical development resembles, in many respects, the method of calculating transonic potential flow proposed by Bristeau, Pironneau, Glowinski, Periaux, Perrier and Poirier, who reformulated the solution of the flow equations as a least squares problem in control theory [4]. Pironneau has also studied the use of control theory for optimum shape design of systems governed by elliptic equations [24].

This paper explores the application of control theory for the design of transonic airfoils in two-dimensional flow. The governing equation is taken to be the transonic potential flow equation, and the profile is generated by conformal mapping from a unit circle. Thus, the control is taken to be the modulus of the mapping function on the boundary. The cost function is taken to be a blend of a measure of the deviation from a desired pressure distribution, and the pressure drag induced by the appearance of shock waves. The equations are developed in the next section. Section 3 outlines the numerical procedures used to solve the corresponding discrete equations. Section 4 presents some computational results which demonstrate the capability of the method to reshape the profile to reduce the pressure drag in transonic flow by a factor of ten. The success of the method for this model problem encourages the belief that it offers a feasible

approach to more complex optimization problems, such as the optimization of the complete wing, or the inclusion of a viscous flow model for design to reduce both pressure and friction drag.

2 Design for potential flow using conformal mapping

Consider the case of two-dimensional compressible inviscid flow. In the absence of shock waves, an initially irrotational flow will remain irrotational, and we can assume that the velocity vector \underline{q} is the gradient of a potential ϕ . In the presence of weak shock waves this remains a fairly good approximation. Let $\underline{\zeta}$, T and S denote vorticity, temperature and entropy. Then, according to Crocco's Theorem, vorticity in steady inviscid iso-energetic flow is associated with entropy production through the relation

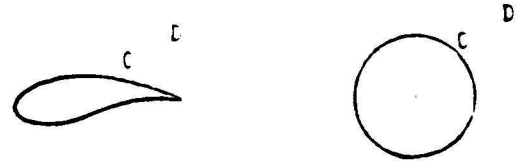


Figure 1: z -plane

σ -plane

$$\underline{q} \times \underline{\zeta} + T \nabla S = 0 \quad (6)$$

Thus, the introduction of a potential is consistent with the assumption of isentropic flow, and shock waves are modelled by isentropic jumps. Let p , ρ , c and M be the pressure, density, speed-of-sound and Mach number q/c . Then the potential flow equation is

$$\nabla \cdot \rho \nabla \phi = 0 \quad (7)$$

where the density is given by

$$\rho = \left\{ 1 + \frac{\gamma - 1}{2} M_\infty^2 (1 - q^2) \right\}^{1/(\gamma - 1)} \quad (8)$$

while

$$p = \frac{\rho^\gamma}{\gamma M_\infty^2}, \quad c^2 = \frac{\gamma p}{\rho} \quad (9)$$

Here M_∞ is the Mach number in the free stream, and the units have been chosen so that p and q have the value unity in the far field. Equation 8 is a consequence of the energy equation in the form

$$\frac{c^2}{\gamma - 1} + \frac{q^2}{2} = \text{constant} \quad (10)$$

Suppose that the domain D exterior to the profile C in the z -plane is conformally mapped on to

the domain exterior to a unit circle in the σ -plane as sketched in Figure 1. Let R and θ be polar coordinates in the σ -plane, and let r be the inverted radial coordinate $1/R$. Also let h be the modulus of the derivative of the mapping function

$$h = \left| \frac{dz}{d\sigma} \right| \quad (11)$$

Now the potential flow equation becomes

$$\frac{\partial}{\partial \theta} (\rho \phi_\theta) + r \frac{\partial}{\partial r} (r \rho \phi_r) = 0 \quad \text{in } D \quad (12)$$

where the density is given by Equation 8, and the circumferential and radial velocity components are

$$u = \frac{r \phi_\theta}{h}, \quad v = \frac{r^2 \phi_r}{h} \quad (13)$$

while

$$q^2 = u^2 + v^2 \quad (14)$$

The condition of flow tangency leads to the Neumann boundary condition

$$v = \frac{1}{h} \frac{\partial \phi}{\partial r} = 0 \quad \text{on } C \quad (15)$$

In the far field, the potential is given by an asymptotic estimate, leading to a Dirichlet boundary condition at $r = 0$ [2].

Suppose that it is desired to achieve a specified velocity distribution q_d on C . Introduce the cost function

$$I = \frac{1}{2} \int_C (q - q_d)^2 d\theta, \quad (16)$$

The design problem is now treated as a control problem where the control function is the mapping modulus h , which is to be chosen to minimize I subject to constraints defined by the flow equations 7-15.

A modification δh to the mapping modulus will result in variations $\delta \phi, \delta u, \delta v$, and $\delta \rho$ to the potential, velocity components and density. The resulting variation in the cost will be

$$\delta I = \int_C (q - q_d) \delta q d\theta, \quad (17)$$

where on C , $q = u$. Also,

$$\delta u = r \frac{\delta \phi_\theta}{h} - u \frac{\delta h}{h}, \quad \delta v = r^2 \frac{\delta \phi_r}{h} - v \frac{\delta h}{h}$$

while according to equations 8 and 14

$$\frac{\partial \rho}{\partial u} = -\frac{\rho u}{c^2}, \quad \frac{\partial \rho}{\partial v} = -\frac{\rho v}{c^2}$$

Hence,

$$\begin{aligned} \delta \rho &= -\frac{\rho}{c^2} (u \delta u + v \delta v) \\ &= \rho \frac{q^2}{c^2} \frac{\delta h}{h} - \frac{\rho}{c^2} \frac{r}{h} (u \delta \phi_\theta + v r \delta \phi_r) \end{aligned} \quad (18)$$

It follows that $\delta \phi$ satisfies

$$L \delta \phi = -\frac{\partial}{\partial \theta} \left(\rho M^2 \phi_\theta \frac{\delta h}{h} \right) - r \frac{\partial}{\partial r} \left(\rho M^2 r \phi_r \frac{\delta h}{h} \right)$$

where

$$\begin{aligned} L &\equiv \frac{\partial}{\partial \theta} \left\{ \rho \left(1 - \frac{u^2}{c} \right) \frac{\partial}{\partial \theta} - \frac{\rho u v}{c^2} r \frac{\partial}{\partial r} \right\} \\ &\quad + r \frac{\partial}{\partial r} \left\{ \rho \left(1 - \frac{v^2}{c} \right) r \frac{\partial}{\partial r} - \frac{\rho u v}{c^2} \frac{\partial}{\partial \theta} \right\} \end{aligned} \quad (19)$$

Then if ψ is any periodic differentiable function which vanishes in the far field,

$$\int_D \frac{\psi}{r^2} L \delta \phi dS = \int_D \rho M^2 \nabla \phi \cdot \nabla \psi \frac{\delta h}{h} dS \quad (20)$$

where dS is the area element $r dr d\theta$, and the right hand side has been integrated by parts.

Now we can augment Equation 17 by subtracting the constraint 20. The auxiliary function ψ then plays the role of a Lagrange multiplier. Substituting for δq and integrating the term

$$\int_C (q - q_d) r \frac{\delta \phi}{h} d\theta$$

by parts, we obtain

$$\begin{aligned} \delta I &= \int_C (q - q_d) q \frac{\delta h}{h} d\theta - \int_C \delta \theta \frac{\partial}{\partial \theta} \left(\frac{q - q_d}{h} \right) d\theta \\ &\quad - \int_D \frac{\psi}{r^2} L \delta \phi dS + \int_D \rho M^2 \nabla \phi \cdot \nabla \psi \frac{\delta h}{h} dS \end{aligned}$$

Now suppose that ψ satisfies the adjoint equation

$$L \psi = 0 \quad \text{in } D \quad (21)$$

with the boundary condition

$$\frac{\partial \psi}{\partial r} = \frac{1}{\rho} \frac{\partial}{\partial \theta} \left(\frac{q - q_d}{h} \right) \quad \text{on } C \quad (22)$$

Then, integrating by parts,

$$\int_D \frac{\psi}{r^2} L \delta \phi dS = - \int_C \rho \psi_r \delta \phi d\theta$$

and

$$\begin{aligned} \delta I &= - \int_C (q - q_d) q \frac{\delta h}{h} d\theta \\ &\quad + \int_D \rho M^2 \nabla \phi \cdot \nabla \psi \frac{\delta h}{h} dS \end{aligned} \quad (23)$$

Here the first term represents the direct effect of the change in the metric, while the area integral represents a correction for the effect of compressibility.

Equation 23 can be further simplified to represent δI purely as a boundary integral because the mapping function is fully determined by the value of its modulus on the boundary. Set

$$\log \frac{dz}{d\sigma} = f + i\beta$$

where

$$f = \log \left| \frac{dz}{d\sigma} \right| = \log h$$

and

$$\delta f = \frac{\delta h}{h}$$

Then f satisfies Laplace's equation

$$\Delta f = 0 \quad \text{in } D$$

and if there is no stretching in the far field, $f \rightarrow 0$. Thus,

$$\Delta \delta f = 0 \quad \text{in } D$$

and $\delta f \rightarrow 0$ in the far field.

Introduce another auxiliary function P which satisfies

$$\Delta P = \rho M^2 \nabla \phi \cdot \nabla \psi \quad \text{in } D \quad (24)$$

and

$$P = 0 \quad \text{on } C \quad (25)$$

Then, the area integral in Equation 23 is

$$\int_D \Delta P \delta f dS = \int_C \delta f \frac{\partial P}{\partial r} d\theta - \int_D \Delta P \delta f dS$$

and finally

$$\delta I = \int_C g \delta f d\theta \quad (26)$$

where

$$g = \frac{\partial P}{\partial r} - (q - qa) q \quad (27)$$

This suggests setting

$$\delta f = -\lambda g$$

so that if λ is a sufficient small positive number

$$\delta I = -\lambda \int_C g^2 d\theta < 0$$

Arbitrary variations in δf cannot, however, be admitted. The condition that $f \rightarrow 0$ in the far field, and also the requirement that the profile should be closed, imply constraints which must be satisfied by f on the boundary C . Suppose that $\log \left(\frac{dz}{d\sigma} \right)$ is expanded as a power series

$$\log \left(\frac{dz}{d\sigma} \right) = \sum_{n=0}^{\infty} \frac{c_n}{\sigma^n} \quad (28)$$

where only negative powers are retained because otherwise $\frac{dz}{d\sigma}$ would become unbounded for large σ . The condition that $f \rightarrow 0$ as $\sigma \rightarrow \infty$ implies

$$c_0 = 0$$

Also, the change in z on integration around circuit a is

$$\Delta z = \int \frac{dz}{d\sigma} d\sigma = 2\pi i c_1$$

so the profile will be closed only if

$$c_1 = 0$$

On C , Equation 28 reduced to

$$\begin{aligned} f_C + i\beta_C &= \sum_{n=0}^{\infty} (a_n \cos n\theta - b_n \sin n\theta) \\ &+ i \sum_{n=0}^{\infty} (b_n \cos n\theta - a_n \sin n\theta) \end{aligned}$$

Thus a_n and b_n are the Fourier coefficients of f_C , and these constraints reduce to

$$a_0 = 0, \quad a_1 = 0, \quad b_1 = 0$$

In order to satisfy these constraints, we can project g onto the admissible subspace for f_C by setting

$$\tilde{g} = g - A_0 - A_1 \cos \theta - B_1 \sin \theta \quad (29)$$

where

$$\begin{aligned} A_0 &= \frac{1}{2\pi} \int_C g d\theta, \\ A_1 &= \frac{1}{\pi} \int_C g \cos \theta d\theta, \\ B_1 &= \frac{1}{\pi} \int_C g \sin \theta d\theta, \end{aligned} \quad (30)$$

Then,

$$\int_C (g - \tilde{g}) \tilde{g} d\theta = 0$$

and if we take

$$\delta f = \lambda \tilde{g}$$

it follows that to first order

$$\begin{aligned} \delta I &= -\lambda \int_C g \tilde{g} d\theta = -\lambda \int_C (\tilde{g} + g - \tilde{g}) g d\theta \\ &= -\lambda \int_C \tilde{g}^2 d\theta < 0 \end{aligned}$$

If the flow is subsonic, this procedure should converge toward the desired speed distribution since the solution will remain smooth, and no unbounded derivatives will appear. If, however, the flow is transonic, one must allow for the appearance of shock waves

in the trial solutions, even if q_d is smooth. Then $q - q_d$ is not differentiable. This difficulty can be circumvented by a more sophisticated choice of the cost function. Consider the choice

$$I = \frac{1}{2} \int_C \left(\lambda_1 S^2 + \lambda_2 \left(\frac{dS}{d\theta} \right)^2 \right) d\theta \quad (31)$$

where λ_1 and λ_2 are parameters, and the periodic function $S(\theta)$ satisfies the equation

$$\lambda_1 S - \lambda_2 \frac{d^2 S}{d\theta^2} = q - q_d \quad (32)$$

Then,

$$\begin{aligned} \delta I &= \int_C \left(\lambda_1 S \delta S + \lambda_2 \frac{dS}{d\theta} \frac{d}{d\theta} \delta S \right) d\theta \\ &= \int_C S \left(\lambda_1 \delta S + \lambda_2 \frac{d^2}{d\theta^2} \delta S \right) d\theta \\ &= \int_C S \delta q d\theta \end{aligned}$$

Thus, S replaces $q - q_d$ in the previous formulas, and if one modifies the boundary condition 22 to

$$\frac{\partial \psi}{\partial r} = \frac{1}{\rho} \frac{\partial}{\partial \theta} \left(\frac{S}{h} \right) \quad \text{on } C \quad (33)$$

the formula for the gradient becomes

$$g = \frac{\partial P}{\partial r} - S q \quad (34)$$

instead of Equation 27. Then, one modifies f by a step $-\lambda \tilde{g}$ in the direction of the projected gradient as before.

The final design procedure is thus as follows. Choose an initial profile and corresponding mapping function f . Then:

1. Solve the flow equations (7-15) for ϕ, u, v, q, ρ .
2. Solve the ordinary differential equation 32 for S .
3. Solve the adjoint equation (21) for ψ subject to the boundary condition (33).
4. Solve the auxiliary Poisson equation (24) for P .
5. Evaluate

$$g = \frac{\partial P}{\partial r} - S q$$

on C , and find its projection \tilde{g} onto the admissible subspace of variations according to Equations 29 and 31.

6. Correct the boundary condition mapping function f_C by

$$\delta f = \lambda \tilde{g}$$

and return to step 1.

3 Numerical Procedures

The practical realization of the design procedure depends on the availability of sufficiently fast and accurate numerical procedures for the implementation of the essential steps, in particular the solution of both the flow and the adjoint equations. If the numerical procedures are not accurate enough, the resulting errors in the gradient may impair or prevent the convergence of the descent procedure. If the procedures are too slow, the cumulative computing time may become excessive. In this case, it was possible to build the design procedure around the author's computer program FLO36, which solves the transonic potential flow equation in conservation form in a domain mapped to the unit disk. The solution is obtained by a very rapid multigrid alternating direction method. The original scheme is described in Reference [25]. The program has been much improved since it was originally developed, and well converged solutions of transonic flows on a mesh with 128 cells in the circumferential direction and 32 cells in the radial direction are typically obtained in 5-20 multigrid cycles. The scheme uses artificial dissipative terms to introduce upwind biasing which simulates the rotated difference scheme [2], while preserving the conservation form. The alternating direction method is a generalization of conventional alternating direction methods, in which the scalar parameters are replaced by upwind difference operators to produce a scheme which remains stable when the type changes from elliptic to hyperbolic as the flow becomes locally supersonic [25]. The conformal mapping is generated by a power series of the form of Equation 28 with an additional term

$$\left(1 - \frac{\epsilon}{\pi} \right) \log \left(1 - \frac{1}{\sigma} \right)$$

to allow for a wedge angle ϵ at the trailing edge. The coefficients are determined by an iterative process with the aid of fast Fourier transforms [2].

The adjoint equation has a form very similar to the flow equation. While it is linear in its dependent variable, it also changes type from elliptic in subsonic zones of the flow to hyperbolic in supersonic zones of the flow. Thus, it was possible to adapt exactly the same algorithm to solve both the adjoint and the flow equations, but with reverse biasing of the difference operators in the downwind direction in the adjoint equation, corresponding to the reversed direction of the zone-of-dependence. The Poisson equation (24) is solved by the Buneman algorithm.

An alternative procedure would be to calculate the exact derivative of the cost function with respect to the control directly from the discrete equations used

to approximate the transonic potential flow equation. This would eliminate discretization errors in the estimate of the gradient at the expense of more complicated formulas with correspondingly increased computing costs, and it was therefore rejected.

4 Results

The capability of the scheme in practice has been verified by a variety of numerical experiments. First, in order to illustrate the use of the scheme to solve the inverse problem of designing profiles for a given pressure distribution, Figures 2 and 3 show the results of design calculations in which the target pressure distributions correspond to the Korn and NACA 64A410 airfoils. For the Korn design, the initial profile was the NACA 64A410, and a shock free design essentially indistinguishable from the Korn airfoil was obtained in 25 iterations. Figure 3 illustrates the reverse process. Starting from the Korn airfoil, a profile indistinguishable from the NACA 64A410 was recovered in 15 iterations.

It is interesting to speculate on the possibility of designing profiles to realize the smooth Korn pressure distribution at Mach numbers higher than the Korn design point of Mach 0.75. Figures 4 and 5 show the results of attempts to realize such designs at Mach numbers of 0.8 and 0.82. Although the results show a smooth pressure distribution on the surface, these flows in fact contain embedded shocks detached from the surface, and these is a corresponding pressure drag. At Mach 0.82, a very strong shock wave is located above the reversed camber region towards the rear of the top surface. These flows are extremely sensitive to small variations in the geometry, and required 200 to 400 iterations to converge.

These examples show that the attainment of a smooth surface pressure distribution is not sufficient to guarantee low pressure drag, because of the possibility that detached shock waves may still appear in the flow field. To prevent this, one may include the drag coefficient in the cost function so that Equation 31 is replaced by the form

$$I = \frac{1}{2} \int_C \left(\lambda_1 S^2 + \lambda_2 \left(\frac{dS}{d\theta} \right)^2 \right) d\theta + \beta CD$$

where S is the smoothed deviation from the target speed given by Equation 32, and β is a parameter which may be varied to alter the trade-off between drag reduction and deviation from the desired pressure distribution. Representing the drag as

$$D = \int_C (p - p_\infty) dy$$

the procedure of Section 2 may be used to determine the gradient of the augmented cost function by solving the adjoint equation with a correspondingly modified boundary condition. Figure 6 shows the result of including a drag penalty for the case of the Korn target pressure distribution at Mach 0.82. In comparison with Figure 4, it can be seen that the drag coefficient is reduced from 0.0089 to 0.0010, while the lift coefficient is very slightly reduced from 0.645 to 0.630.

The remaining examples illustrates the use of the method in a pure drag reduction mode. In this case, the target pressure distribution is taken to be the actual pressure distribution of the initial profile predicted by the numerical solution of the flow equation. The addition of a drag penalty now causes the method to reshape the profile to reduce its drag. The inclusion of the initial pressure distribution as a target forces the method to generate a profile as a life coefficient close to that of the initial profile, and avoids the pitfall of using the optimization procedure to discover that a flat plate at zero-angle of attach has zero drag. The program also has an option to generate solutions at a fixed lift coefficient while allowing the angle-of-attack to float. Figure 7 shows a redesign of the RAE 2822 at Mach 0.730 with an initial lift coefficient of 1.05. In this case the design was essentially frozen after 6 cycles, and the strength of the shock wave was reduced at each cycle, with the final result that the drag coefficient was reduced from 0.0170 to 0.016.

The question arises whether optimization at one design point might not lead to an improvement in a very narrow band of conditions at the expense of impaired off-design performance. The optimization procedure is not, however, limited to a single design point. If one takes the sum of cost functions for several design points, the formulas for the gradient are additive, and the method may be used to seek a compromise design. Figure 8 illustrates the result of such an experiment. The RAE 2822 was again used as the initial profile, with three design targets, CL 1.05 at Mach 0.730, CL 0.95 at Mach 0.740, and CL 0.85 at Mach 0.750. These three conditions all produce severe shock waves of roughly equal strength, with initial drag coefficients of 0.0173, 0.0156, and 0.0149. The objective is now to reduce the sum of the three drag coefficients. After 9 cycles, the coefficients are 0.0055, 0.0023, and 0.0006. The sum of the drag coefficients is thus reduced from 0.0478 to 0.0084. It can also be seen that an almost shock free results is obtained at Mach 0.750. The convergence of the method tends to be more erratic when seeking a compromise design with additive cost functions of this kind. If a very low value of drag is attained at

one of the design points, this makes a small contribution to the gradient, so in the following cycle the modification to reduce the drag at the other design points may cause the drag at the first design point to bounce back up again.

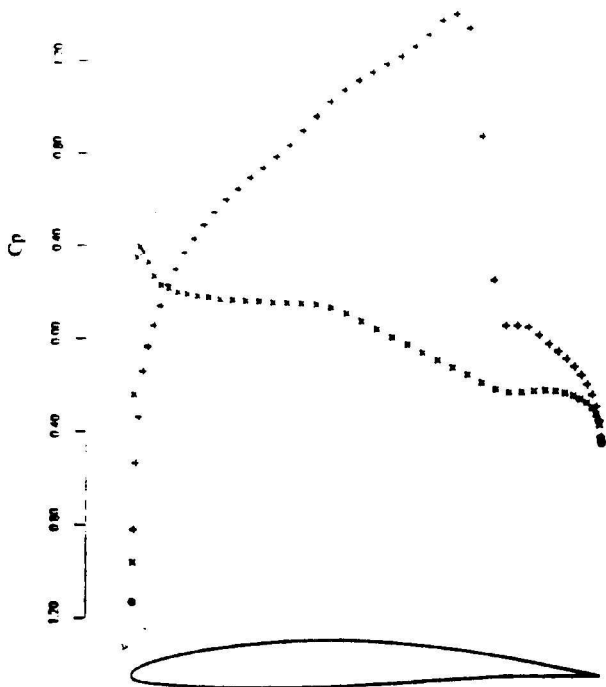
5 Conclusion

If optimization is to have a real impact on design, it will be necessary to treat more complete models of the flow, at least including viscous effects in the boundary layer, and to treat three-dimension configurations. The present study of two-dimensional inviscid flow provides a useful model, however, to test the feasibility of using control theory as a design tool. The experience gained with it reinforces the belief that control theory offers an effective approach to design. In comparison with more straight forward optimization methods, the use of the adjoint equation to estimate the gradient greatly reduces computing costs. A similar formulation can be used for the optimization of complete three-dimensional wings, using coordinate transformations to generate the shape, and one may also modify the adjoint equations to allow for a boundary layer. Intelligent optimization methods ought, in due course, to play an increasingly important role in the design process, with real pay-offs both in reduced design costs and in increased efficiency of the final project.

References

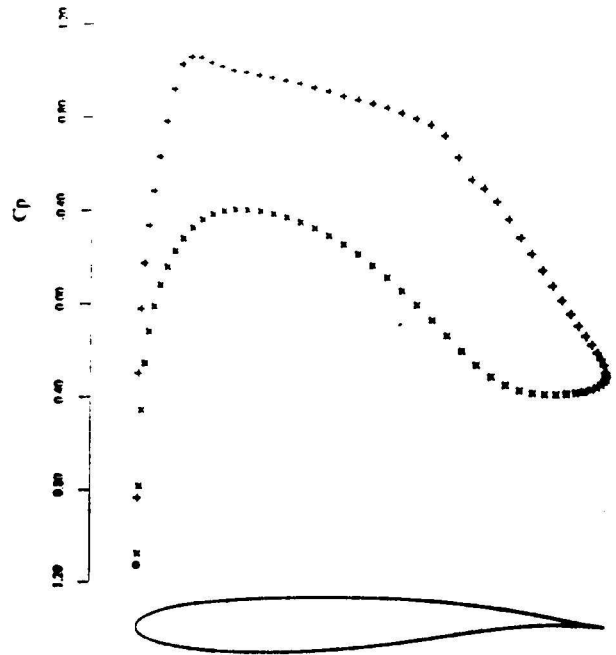
- [1] Murman, E.M. and Cole, J.D., "Calculation of Plane Steady Transonic Flows", AIAA Journal, Vol. 9, 1971, pp. 114-121.
- [2] Jameson, A., "Iterative Solution of Transonic Flows Over Airfoils and Wings", Including Flows at Mach 1, Comm. Pure. Appl. Math, Vol. 27, 1974, pp. 283-309.
- [3] Jameson, A. and Caughey, D.A., "A Finite Volume Method for Transonic Potential Flow Calculations", Proc. AIAA 3rd Computational Fluid Dynamics Conference, Albuquerque, 1977, pp. 35-54.
- [4] Bristeau, M.O., Pironneau, O., Glowinski, R., Periaux, J., Perrier, P., and Poirier, G., "On the Numerical Solution of Nonlinear Problems in Fluid Dynamics by Least Squares and Finite Element Methods (II). Application to Transonic Flow Simulations", Proc. 3rd International Conference on Finite Elements in Nonlinear Mechanics, FENOMECH 84, Stuttgart, 1983, edited by J. St. Doltsinis, North Holland, 1985, pp. 363-394.
- [5] Jameson, A., Schmidt, W., and Turkel, E., "Numerical Solution of the Euler Equations by Finite Volume Methods Using Runge-Kutta Time Stepping Schemes", AIAA Paper 81-1259, AIAA 14th Fluid Dynamics and Plasma Dynamics Conference, Palo Alto, 1981.
- [6] Ni, Ron Ho, "A multiple Grid Scheme for Solving the Euler Equations", AIAA Journal, Vol. 20, 1982, pp. 1565-1571.
- [7] Pulliam, T.H. and Steger, J.L., "Recent Improvements in Efficiency, Accuracy and Convergence for Implicit Approximate Factorization Algorithms", AIAA Paper 85-0360, AIAA 23rd Aerospace Sciences Meeting, Reno, January 1985.
- [8] MacCormack, R.W., "Current Status of Numerical Solutions of the Navier-Stokes Equations", AIAA Paper 85-0032, AIAA 23rd Aerospace Sciences Meeting, Reno, January 1985.
- [9] Jameson, A, Baker, T.J. and Weatherill, N.P., "Calculation of Inviscid Transonic Flow Over a Complete Aircraft", AIAA Paper 86-0103, AIAA 24th Aerospace Sciences Meeting, Reno, January 1986.
- [10] Jameson, A., "Successes and Challenges in Computational Aerodynamics", AIAA Paper 87-1184-CP, 8th Computational Fluid Dynamics Conference, Hawaii, 1987.
- [11] Lighthill, M.J., "A New Method of Two Dimensional Aerodynamic Design", ARC, Rand M 2112, 1945.
- [12] McFadden, G.B., "An Artificial Viscosity Method for the Design of Supercritical Airfoils", New York University Report COO-3077-158, 1979.
- [13] Taverna, F., "Advanced Airfoil Design for General Aviation Propellers", AIAA Paper 83-1791, 1983.
- [14] Garabedian, P. and McFadden, G., "Computational Fluid Dynamics of Airfoils and Wings", Proc. of Symposium on Transonic, Shock, and Multi-dimensional Flows, Madison, 1981, Meyer, R., ed., Academic Press, New York, 1982, pp. 1-16.
- [15] Tranen, J.L., "A Rapid Computer Aided Transonic Airfoil Method", AIAA Paper 74-501, 1974.

- [16] Volpe, G. and Melnik, R.E., “The Design of Transonic Aerofoils by a Well Posed Inverse Method”, *Int. J. Numerical Methods in Engineering*, Vol. 22, 1986, pp. 341-361.
- [17] Henne, P.A., “An Inverse Transonic Wing Design Method”, AIAA Paper 80-0330, 1980.
- [18] Garabedian, P.R. and Korn, D.G., “Numerical Design of Transonic Airfoils”, *Proc. SYNPADE 1970*, Hubbard, B., ed., Academic Press, New York, 1971, pp. 253-271.
- [19] Giles, M., Drela, M. and Thompkins, W.T., “Newton Solution of Direct and Inverse Transonic Euler Equations”, AIAA Paper 85-1530, *Proc AIAA 7th Computational Fluid Dynamics Conference*, Cincinnati, 1985, pp. 394-402.
- [20] Hicks, R.M. and Henne, P.A., “Wing Design by Numerical Optimization”, AIAA Paper 79-0080, 1979.
- [21] Constantino, G.B., and Holst, T.L., “Numerical Optimization Design of Advanced Transonic Wing Configurations”, NASA Report, T.M. 85950, 1984.
- [22] Jameson, Antony, “Aerodynamic Design via Control Theory”, *J. Scientific Computing*, Vol. 3, 1988, pp. 233-260.
- [23] Lion, Jacques Louis, “Optimal Control of Systems Governed by Partial Differential Equations”, translated by S.K. Mitter, Springer Verlag, New York, 1971.
- [24] Pironneau, Olivier, “Optimal Shape Design for Elliptic Systems”, Springer Verlag, New York, 1984.
- [25] Jameson, Antony, “Acceleration of Transonic Potential Flow Calculations on Arbitrary Meshes by the Multiple Grid Method”, AIAA Paper 79-1458, *Fourth AIAA Computational Fluid Dynamics Conference*, Williamsburg, July 1979.



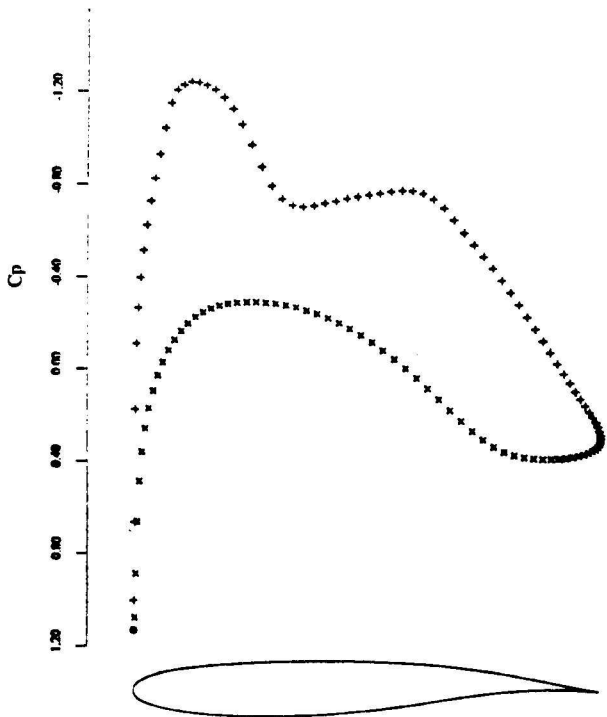
KORN AIRFOIL
MACH 0.750 ALPHA 0.932
CL 0.6209 CD 0.0100 CM -0.1674
GRID 90X16 NCYC 0 RES0.500E-04

Figure 2(a)
Initial Profile



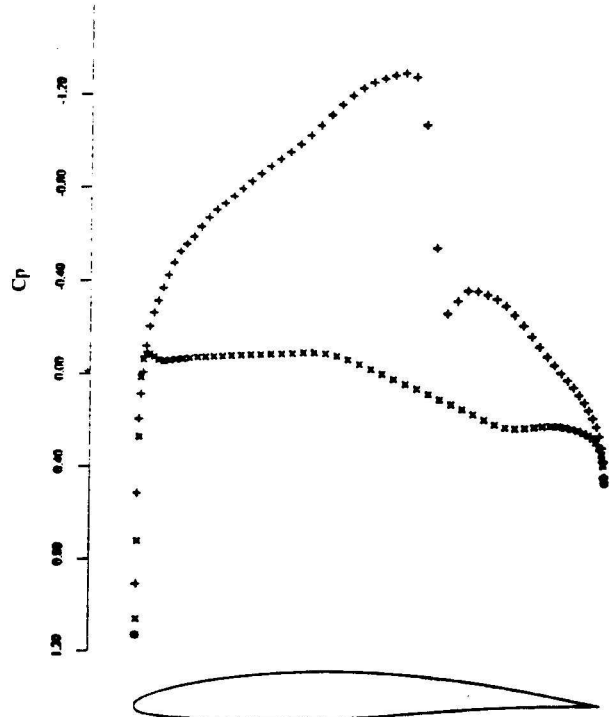
KORN AIRFOIL
MACH 0.750 ALPHA 0.000
CL 0.6274 CD 0.0002 CM -0.1464
GRID 90X16 NCYC 25 RES0.125E-05

Figure 2(b)
Final Design



NACA 64A410
MACH 0.720 ALPHA 0.589
CL 0.6740 CD 0.0004 CM -0.1332
GRID 128X32 NCYC 0 RES0.750E-05

Figure 3(a)
Initial Profile



NACA 64A410
MACH 0.720 ALPHA 0.002
CL 0.6657 CD 0.0039 CM -0.1451
GRID 128X32 NCYC 15 RES0.216E-06

Figure 3(b)
Final Design

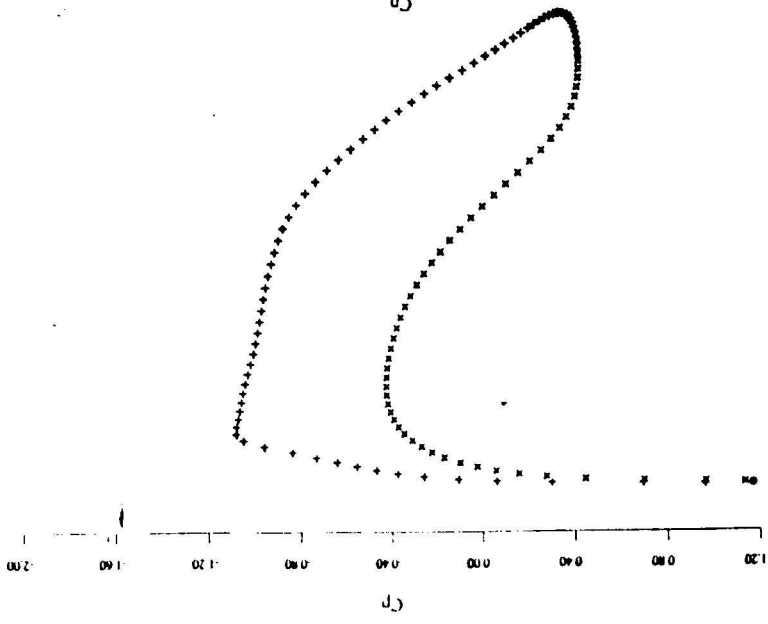


Figure 4
Profile to give Korn pressure distribution at Mach 0.80

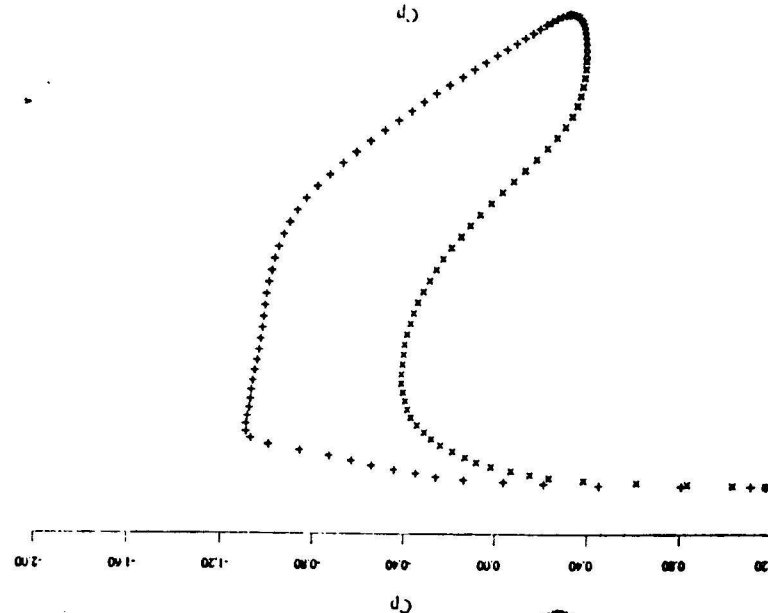


Figure 5
Profile to give Korn pressure distribution at Mach 0.82

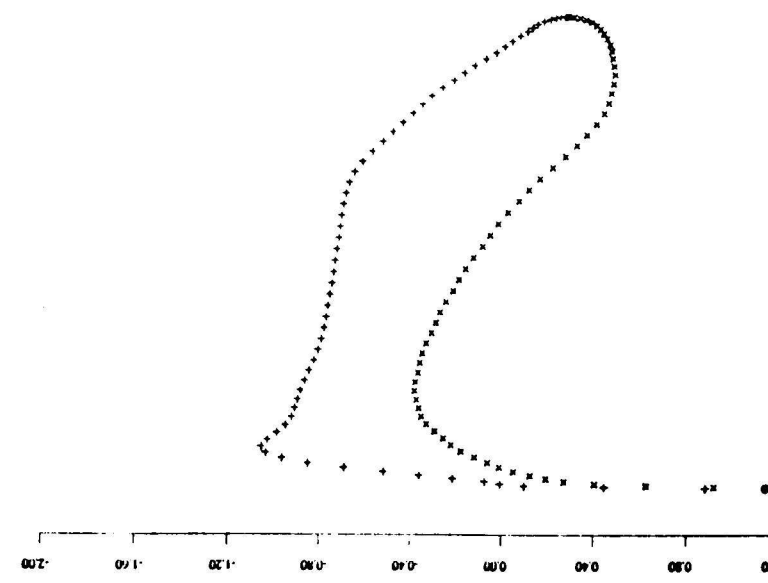
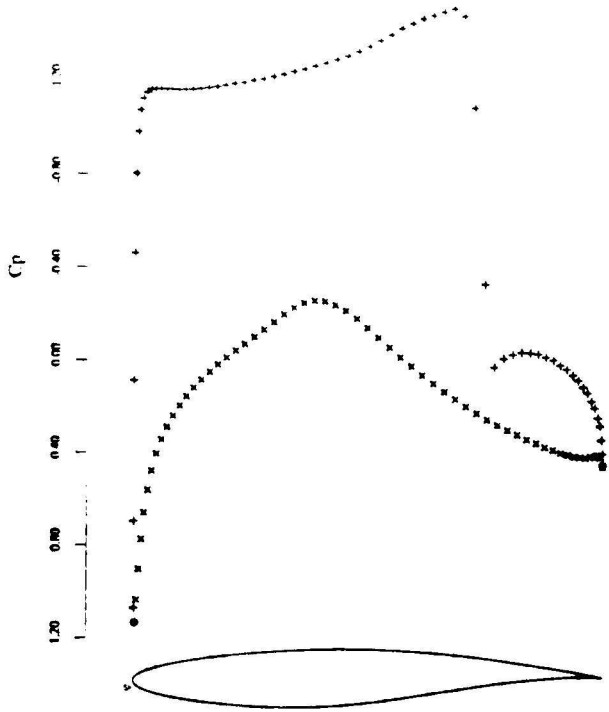
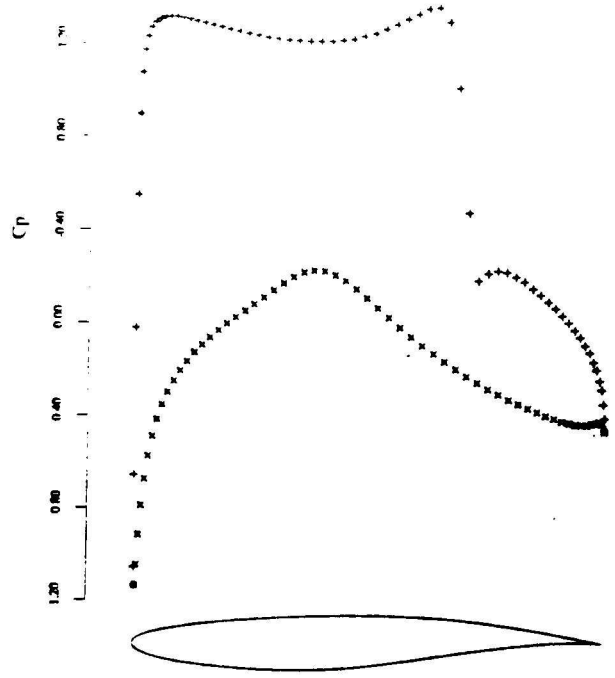


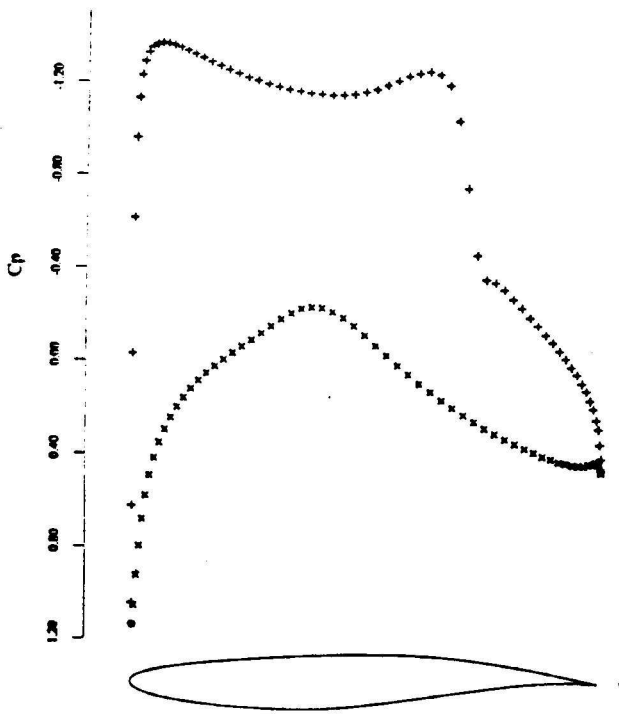
Figure 6
Profile to approach Korn pressure distribution at Mach 0.80 with drag penalty



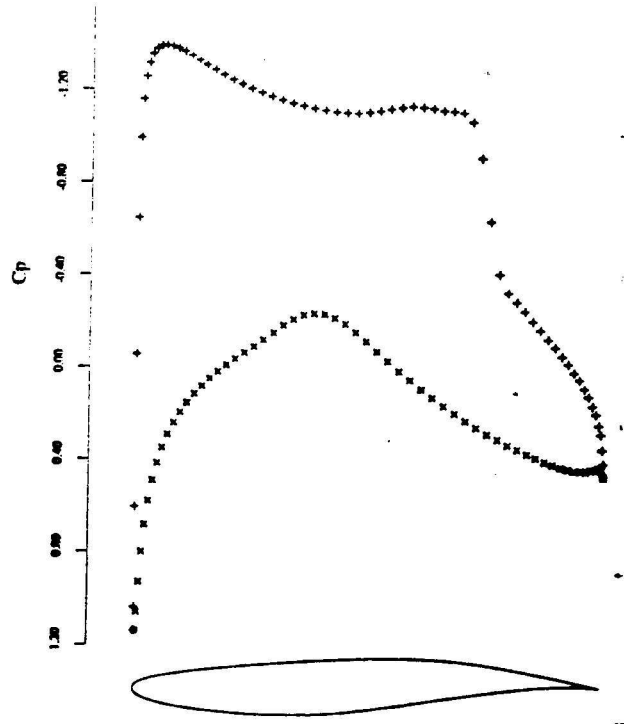
RAE 2822
MACH 0.730 ALPHA 2.000
CL 1.0468 CD 0.0170 CM -0.1745
GRID 128X32 NCYC 0 RES0.358E-05
Figure 7(a) Redesign of RAE 2822
airfoil to reduce drag - Initial Profile



RAE 2822
MACH 0.730 ALPHA 2.002
CL 1.0400 CL 1.0264 CM 1.1606
GRID 128X32 NCYC 2 RES0.368E-06
Figure 7(b) Redesign of RAE 2822 airfoil
to reduce drag - Profile after 2 design cycles



RAE 2822
MACH 0.730 ALPHA 2.045
CL 1.0773 CD 0.0072 CM -0.1551
GRID 128X32 NCYC 4 RES0.997E-06
Figure 7(c) Redesign of RAE 2822 airfoil
to reduce drag - Profile after 4 design cycles



RAE 2822
MACH 0.730 ALPHA 2.016
CL 1.0368 CD 0.0016 CM -0.1699
GRID 128X32 NCYC 6 RES0.634E-06
Figure 7(d) Redesign of RAE 2822 airfoil
to reduce drag - Profile after 6 design cycles

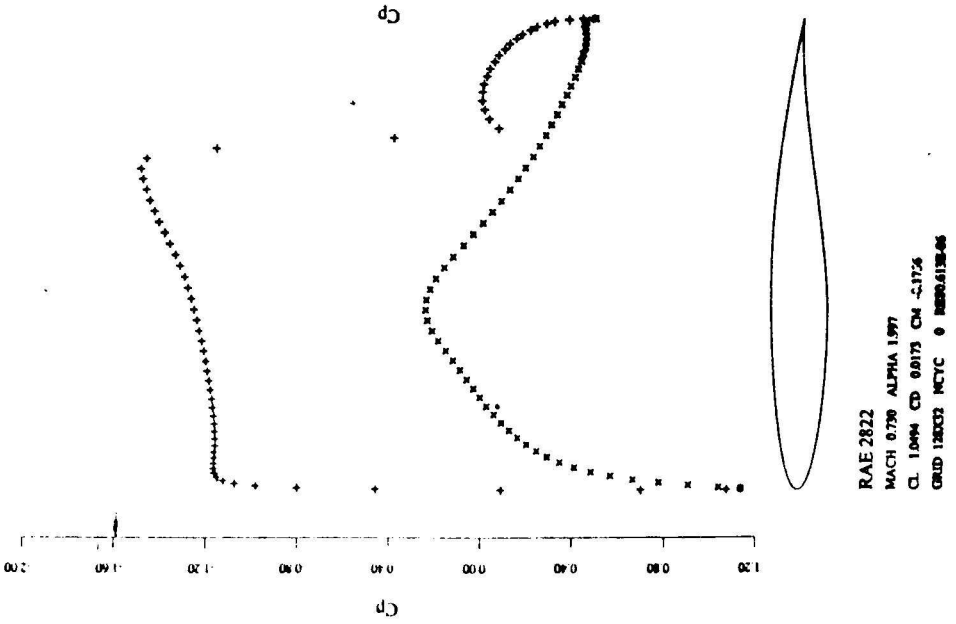


Figure 8(a) Three point redesign of RAE 2822 airfoil - Condition 1 Initial Profile

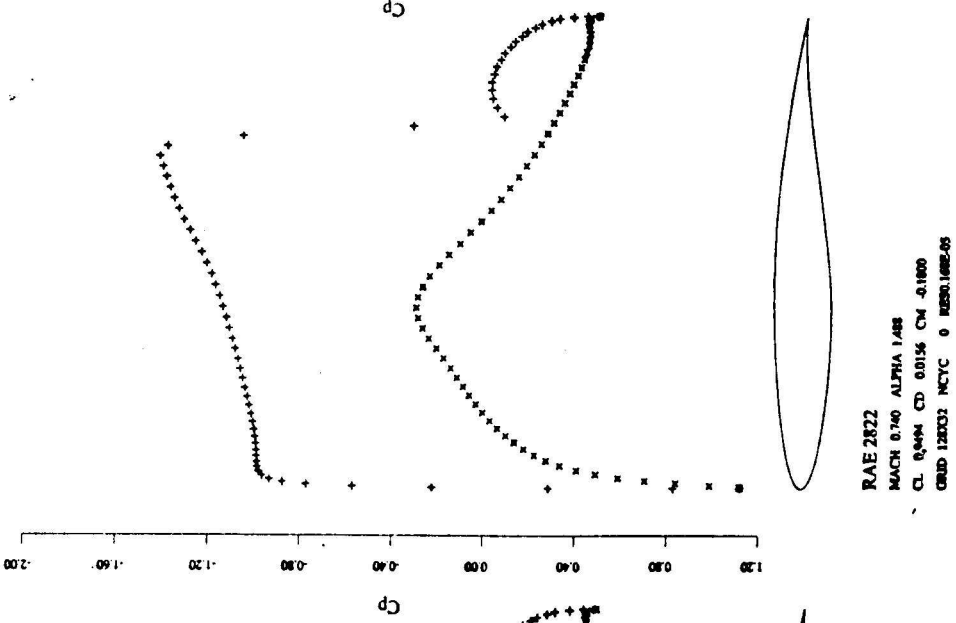


Figure 8(b) Three point redesign of RAE 2822 airfoil - Condition 2 Initial Profile

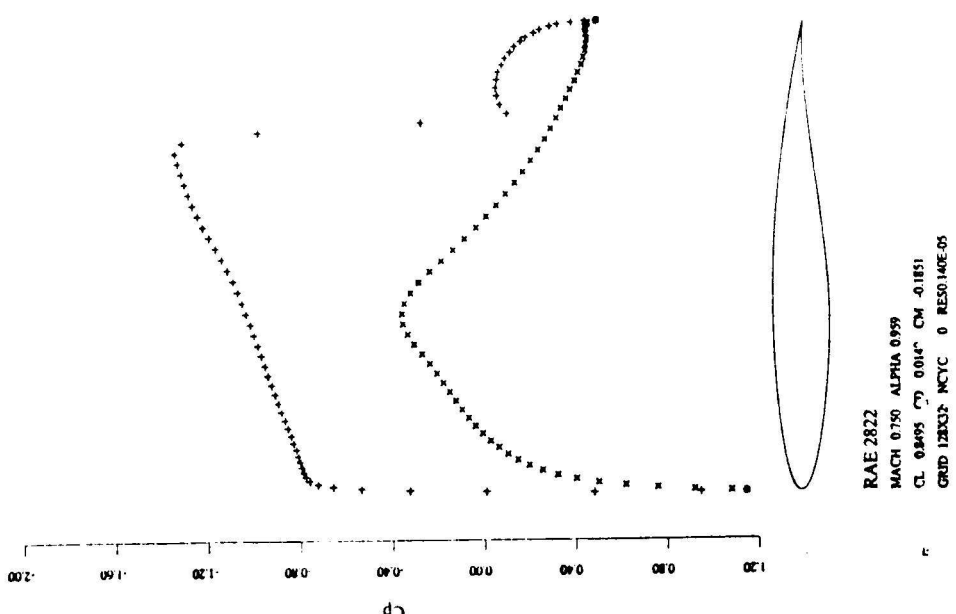


Figure 8(c) Three point redesign of RAE 2822 airfoil - Condition 3 Initial Profile